Archaeological Prospection
Archaeol. Prospect. **19**, 209–218 (2012)
Published online 22 August 2012 in Wiley Online Library
(wileyonlinelibrary.com) DOI: 10.1002/arp.1429

Short Report

The Application of Vegetation Indices for the Prospection of Archaeological Features in Grass-dominated Environments

REBECCA BENNETT*, KATE WELHAM, ROSS A. HILL AND ANDREW L. J. FORD

School of Applied Sciences, Bournemouth University, Talbot Campus, Poole BH12 5BB, UK

ABSTRACT The identification of archaeological remains via the capture of localized soil and vegetation change in aerial imagery is a widely used technique for the prospection of new features. The near infrared (NIR) region has been shown by environmental applications to exhibit the signs of vigour and stress better than reflectance in the visible region, and this has led to interest in the application of digital spectral data for archaeological prospection. In this study we assess quantitatively the application of 12 common vegetation indices to archive Compact Airborne Spectrographic Imager digital spectral data acquisitions from January and May 2001 in a grassland environment. The indices are compared with the true colour composite (TCC), best performing spectral band (711.2 $\pm$ 4.9 nm NIR) and the transcription of the aerial photographic archive. The results of the study illustrate that the calculation of a number of vegetation indices can assist with the identification of archaeological features in spectral data. However, the performance of the indices varies by season and although the features detected are shown to be complementary to those detected by the TCC, few indices out-perform the TCC in terms of feature numbers identified. It was also shown that the Normalised Difference Vegetation Index (NDVI), the most commonly applied index in archaeological prospection to date, performed poorly in comparison to indices such as the Modified Red Edge Simple Ratio Index, Simple Ratio Index and Modified Red Edge Normalized Difference Vegetation Index. It is therefore recommended that the application of appropriate vegetation indices can enhance archaeological feature detection when combined with the TCC but that the calculation of the NDVI alone is insufficient to detect additional features. Copyright © 2012 John Wiley & Sons, Ltd.

Key words: Vegetation indices; grassland; multispectral; CASI; NDVI; archaeology

Introduction

Identifying remains of past human interaction with the landscape using aerial imagery is a long held tenet of archaeological prospection across the world. Traditionally panchromatic or colour photography has been used to identify proxy indications of anthropogenic activity. Some of the most commonly detected proxy features are changes in vegetation growth patterns caused by archaeological features in the top and subsoils (Wilson, 1975; Maxwell, 1983; Brophy and Cowley, 2005; Hejcman *et al*., 2011). These changes are generically referred to as crop marks, as the high susceptibility of many arable crops to stress means these features are frequently, though not exclusively, observed in agricultural crop stands.

Those working with aerial imagery in the historic environment sector are becoming increasingly aware of the importance of the non-visible regions of the spectrum for the detection of archaeological features (see Verhoeven and Doneus, 2011; Verhoeven 2012), leading to a growing number of studies using digital spectral data for archaeological prospection. Initially applications focused on feature detection from satellite imagery of predominantly bare earth conditions in southern Europe and the Middle East (Wilkinson, 1993; Mumford and Parcak, 2002; Gheyle *et al*., 2004; Beck *et al*., 2007; Lasaponara and Masini, 2007). More

* Correspondence to: R. Bennett, School of Applied Sciences, Bournemouth University, Talbot Campus, Poole BH12 5BB, UK. E-mail: rbennett@bournemouth.ac.uk

Received 18 June 2012
Accepted 30 July 2012

recently airborne sensors have been applied successfully to detect direct changes associated with archaeological features in the Mediterranean region where the fraction of soil to vegetation is low and archaeological remains are often stone built and upstanding from the ground surface, resulting in high contrast between background and archaeological spectral response (Rowlands and Sarris, 2007; Pascucci *et al*., 2010; Traviglia and Cottica, 2011). An increasing body of work has illustrated the usefulness of airborne spectral data in temperate zones such as the UK (Donoghue and Shennan, 1988; Winterbottom and Dawson, 2005; Powlesland *et al*., 2006; Challis *et al*., 2009; Bennett *et al*., 2011; Aqdus *et al*., 2012). In contrast to the Mediterranean examples, archaeological features in the UK are more often detected through changes in growth patterns caused to the overlying vegetation rather than direct observations of soil. However, analysis of spectral imagery to date has largely ignored the vegetation indices used in environmental studies, focusing instead on the assessment of true and false colour imagery. In a handful of studies the Normalised Difference Vegetation Index (NDVI) (Rouse *et al*., 1973) has been calculated and noted to be of use for the detection of features (Winterbottom and Dawson, 2005; Challis *et al*., 2009; Aqdus *et al*., 2012), however, the application of this index has not been justified with regard to the aims of the research. The potential of vegetation indices in general to highlight parameters such as plant quality, vigour or stress that are related to localized differences caused by underlying anthropogenic features has been illustrated by work undertaken by Traviglia (2005, 2008) in a Mediterranean context, but has yet to be explored for temperate zones.

This paper presents the results of a quantitative comparison of 12 indices selected due to their proven ability to illustrate biophysical parameters of vegetation, for an area of previously recorded archaeological features on the calcareous grassland of the Salisbury Plain, Wiltshire (latitude 51.27, longitude −1.74). In doing so it provides the first assessment of a range of vegetation indices for archaeological prospection in a temperate environment. The aim of this research was to conduct a quantitative comparison of the detection of archaeological features using vegetation indices and relate these results to the feature detection rates from a true colour composite (TCC), the single best performing band of the spectral data and the archive of archaeological features as recorded from aerial photography in the Wiltshire Historic Environment Record (HER). While the record held in the HER is a collection of the evidence from many aerial photographs over many years and therefore cannot be considered directly comparable to a single spectral collection, it provides a useful baseline to assess the effectiveness of any technique compared with the cumulative information from aerial photography. The evaluation of relative success of these indices when detecting archaeological features in the study area will inform future work.

Method

Two archive airborne multispectral datasets collected using the ITRES Compact Airborne Spectrographic Imager (CASI) in January and May 2001 were used for this study. The CASI data were collected in 14 bands ranging from 440 nm to 891 nm as shown in Table 1 and had a ground resolution of 1.5 m. The data were geometrically and atmospherically corrected by the Environment Agency of England and Wales (henceforth EA) prior to acquisition by this project and no further preprocessing was applied.

Over 150 vegetation indices have been published in remote sensing literature, many based on the premise that algebraic combination of spectral bands can highlight useful attributes of vegetation health and growth better than the study of either individual bands or true/false colour RGB images (Ray, 1994). As so little work has been done to establish the use of vegetation

Table 1. Wavelengths of the vegetation bandset of all the digital spectral data supplied for the Everleigh study area.

CASI band	Wavelength range (nm)	Mid-point wavelength (nm)	Interpretation
1	446.2 ± 6.6	446.2	Blue vegetation response
2	470.1 ± 6.6	470.1	Blue vegetation response
3	490.4 ± 6.7	490.4	Green vegetation response
4	550.1 ± 6.7	550.1	Green vegetation maximum
5	671.1 ± 6.8	671.1	Red vegetation absorption maximum
6	683.5 ± 4.0	683.5	Red edge
7	700.7 ± 5.9	700.7	Red edge
8	711.2 ± 4.9	711.2	Red edge
9	721.7 ± 5.9	721.7	Red edge
10	751.3 ± 6.8	751.3	Near infrared plateau
11	763.7 ± 4.0	763.7	Vegetation reflection
12	780.9 ± 5.9	780.9	Water absorption
13	860.2 ± 6.8	860.2	Near infrared plateau
14	880.2 ± 11.6	880.2	Near infrared plateau

DOI: 10.1002/arp

Table 2. Details of the vegetation indices applied in this study.

Index	Abbreviation	Formula	Category	Description
Normalized Difference Vegetation	NDVI	$\mathrm{NVDI} = \frac{\rho_{\mathrm{NIR}} - \rho_{\mathrm{RED}}}{\rho_{\mathrm{NIR}} + \rho_{\mathrm{RED}}}$	Broadband greenness	Normalized difference of green leaf scattering in near infrared and chlorophyll absorption in RED (Rouse *et al*., 1973)
Simple Ratio	SRI	$\mathrm{SR} = \frac{\rho_{\mathrm{NIR}}}{\rho_{\mathrm{RED}}}$	Broadband greenness	Ratio of green leaf scattering in near infrared and chlorophyll absorption in RED (Tucker, 1979)
Enhanced Vegetation I	EVI	$\mathrm{EVI} = 2.5\left(\frac{\rho_{\mathrm{NIR}} - \rho_{\mathrm{RED}}}{\rho_{\mathrm{NIR}} + 6\rho_{\mathrm{RED}} - 7.5\rho_{\mathrm{BLUE}} + 1}\right)$	Broadband greenness	An enhancement on the NDVI to better account for soil background and atmospheric aerosol effects (Heute *et al*., 1997)
Atmospherically Resistant Vegetation	ARVI	$\mathrm{ARVI} = \frac{\rho_{\mathrm{NIR}} - (2\rho_{\mathrm{RED}} - \rho_{\mathrm{BLUE}})}{\rho_{\mathrm{NIR}} + (2\rho_{\mathrm{RED}} - \rho_{\mathrm{BLUE}})}$	Broadband greenness	An enhancement of the NDVI to better account for atmospheric scattering (Kaufman and Tanre, 1996)
Red Edge Normalized Difference Vegetation	RENDVI	$\mathrm{NVDI}_{705} = \frac{\rho_{750} - \rho_{705}}{\rho_{750} + \rho_{705}}$	Narrowband greenness	A modification of the NDVI using reflectance measurements along the red edge (Gitelson and Merzlyak, 1994; Sims and Gamon, 2002)
Modified Red Edge Simple Ratio	MRESRI	$\mathrm{mSR}_{705} = \frac{\rho_{750} - \rho_{445}}{\rho_{705} - \rho_{445}}$	Narrowband greenness	A ratio of reflectance along the red edge with blue reflection correction (Datt, 1999; Sims and Gamon, 2002)
Modified Red Edge Normalized Difference Vegetation	MRENDVI	$\mathrm{mNDVI}_{705} = \frac{\rho_{750} - \rho_{705}}{\rho_{750} + \rho_{705} - 2\rho_{445}}$	Narrowband greenness	A modification of the Red Edge NDVI using blue to compensate for scattered light (Datt, 1999; Sims and Gamon, 2002)
Red Edge Position	REPI	$\mathrm{REP} = 700 + 40\left[\frac{R_{\mathrm{red\ edge}} - R_{700}}{R_{740} - R_{700}}\right]$	Narrowband greenness	The location of the maximum derivative in near-infrared transition, which is sensitive to chlorophyll concentration (Curran *et al*., 1995)
Structure Insensitive Pigment	SIPI	$\mathrm{SIPI} = \frac{\rho_{800} - \rho_{445}}{\rho_{800} - \rho_{680}}$	Light use efficiency	A reflectance measurement designed to maximize the sensitivity of the index to the ratio of bulk carotenoids (e.g. alpha-carotene and beta-carotene) to chlorophyll while decreasing sensitivity to variation in canopy structure (e.g. leaf area index) (Penuelas *et al*., 1995)
Plant Senescence Reflectance	PSRI	$\mathrm{PSRI} = \frac{\rho_{680} - \rho_{500}}{\rho_{750}}$	Dry or senescent carbon	Designed to maximize the sensitivity of the index to the ratio of bulk carotenoids (e.g. alpha-carotene and beta-carotene) to chlorophyll. (Merzlyak *et al*., 1999)
Anthocyanin Reflectance 1	ARI1	$\mathrm{ARI1} = \left(\frac{1}{\rho_{550}}\right) - \left(\frac{1}{\rho_{700}}\right)$	Leaf pigments	Changes in green absorption relative to red indicate leaf anthocyanins. (Gitelson *et al*., 2001)
Anthocyanin Reflectance 2	ARI2	$\mathrm{ARI2} = \rho_{800}\left[\left(\frac{1}{\rho_{550}}\right) - \left(\frac{1}{\rho_{700}}\right)\right]$	Leaf pigments	A variant of the ARI1, which is sensitive to changes in green absorption relative to red, indicating leaf anthocyanins. (Gitelson *et al*., 2001)

DOI: 10.1002/arp

indices for prospection of biophysical parameters relating to archaeological features, guidance was taken from the selection of indices made by Asner (2008). The indices that are potentially appropriate to identifying vegetation stress caused by archaeological features can be grouped into five categories: broadband greenness, narrowband greenness, light use efficiency, dry or senescent carbon and leaf pigments, as detailed in Table 2. All indices are given in full in Table 2, but are referred to by their acronyms in the text.

In previous work by the authors, each band of the CASI data was assessed for its ability to detect

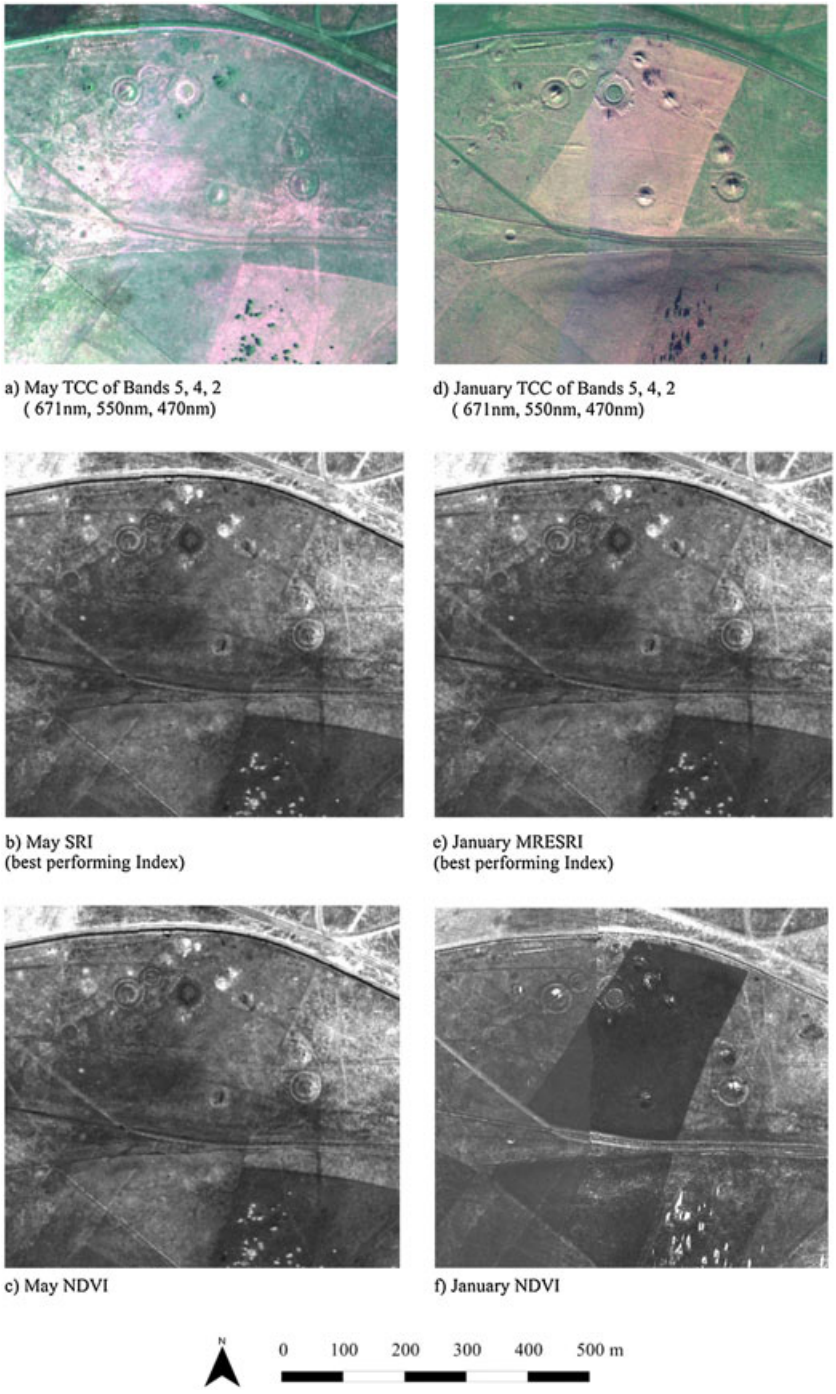

Figure 1. Examples of imagery used in the study: (a) May, TCC; (b) May, SRI; (c) May, NDVI; (d) January, TCC; (e) January, MRESRI; (d) January, NDVI. This figure is available in colour online at wileyonlinelibrary.com/journal/arp.

DOI: 10.1002/arp

archaeological features, and the near infrared (NIR) range of 711.2 ± 4.9 nm (band 8) was shown to be the most useful for feature detection (Bennett, 2012). The vegetation indices were calculated using ENVI 4.7 with the selection of bands that is standard to the software, while the TCC was composed of bands 5 (~671 nm), 4 (~550 nm) and 2 (~490 nm). Archaeological features were then mapped as a vector layer indicating the location and extent from each image following National Mapping Programme protocol for aerial photograph transcription (English Heritage, 2006) at a scale of 1:4000 or less. Examples of imagery are shown in Figure 1. Length was automatically calculated for each vector transcribed and, on comparison of the digitized vector data with the Wiltshire HER record, a maximum detected length from each feature was calculated. The feature lengths recorded by each visualization technique were then converted to a percentage of the maximum detected by any method. This measure was termed average percentage feature length (APFL) of all features in a given visualization. Thus both binary visibility (present or not present) and percentage recovery were measured as an indication of the detection rate of archaeological features in each visualization.

Results

The number of features mapped from each of the vegetation indices for both spectral datasets are shown in Figures 2 (January) and 3 (May). The figures are illustrated alongside the number of known archaeological features in the study area (Wiltshire HER) and the number mapped from the TCC image and most sensitive single band (ca. 711 nm). To illustrate the depiction of archaeological features typical in this environment, a field system of lynchets and banks that runs through three different land-use types is shown in Figure 4.

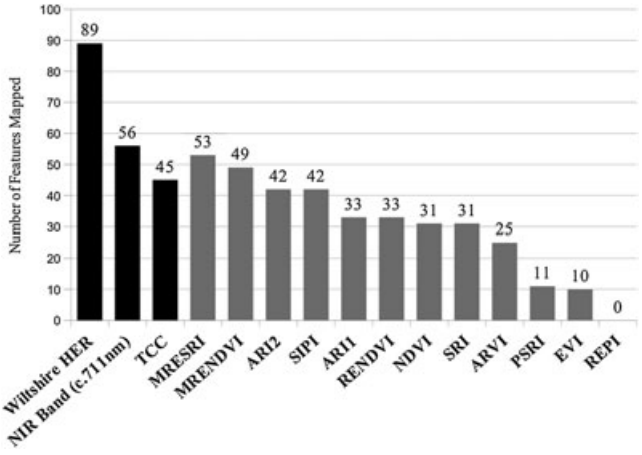

Figure 2. Relative feature detection rates from the vegetation indices applied to the January spectral data.

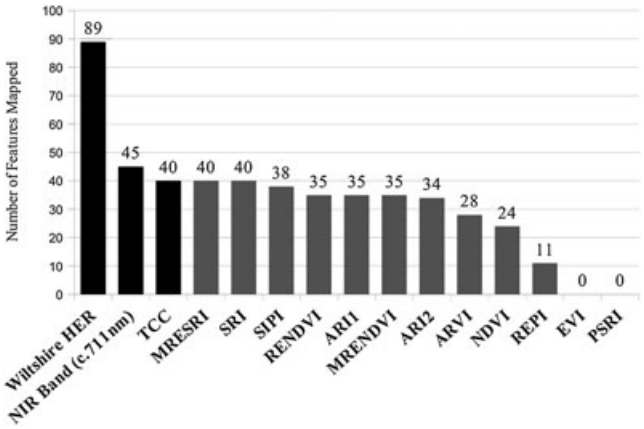

Figure 3. Relative feature detection rates from the vegetation indices applied to the May spectral data.

The clearest result of the study is that the single NIR band of the spectral data outperformed both the TCC and vegetation indices in the January and May data; illustrating the heightened sensitivity of the NIR to changes in plant growth in this environment. This is also highlighted by the fact that in both datasets the TCC recovered fewer of the features known from the aerial photographic archive than the best performing NIR band. It was also shown that a number of vegetation indices can be used to detect archaeological features in the grass dominated environment of the study area. The generally lower feature recovery in the spectral data is unsurprising given its lower spatial resolution when compared with the aerial photography and the fact that the HER archive covers more than 50 yr of data acquisitions at different times of year and under different crop conditions.

The analysis shows that the relative performance of the vegetation indices in comparison with the TCC and single best band varies by season. For the January data, both the MRESRI and the MRENDVI were seen to provide better binary and APFL detection of features than the TCC (Figures 2 and 5). This was not the case for the May data where no index outperformed the TCC in terms of number of features detected (Figure 3), but the MRESRI and SRI had a slightly higher APFL (Figure 6). This concurs with the results of Verhoeven *et al*. (2009), who tested the performance of the SRI created using NIR photography. Of particular note in both datasets is the relatively poor performance of the NDVI, ranking

DOI: 10.1002/arp

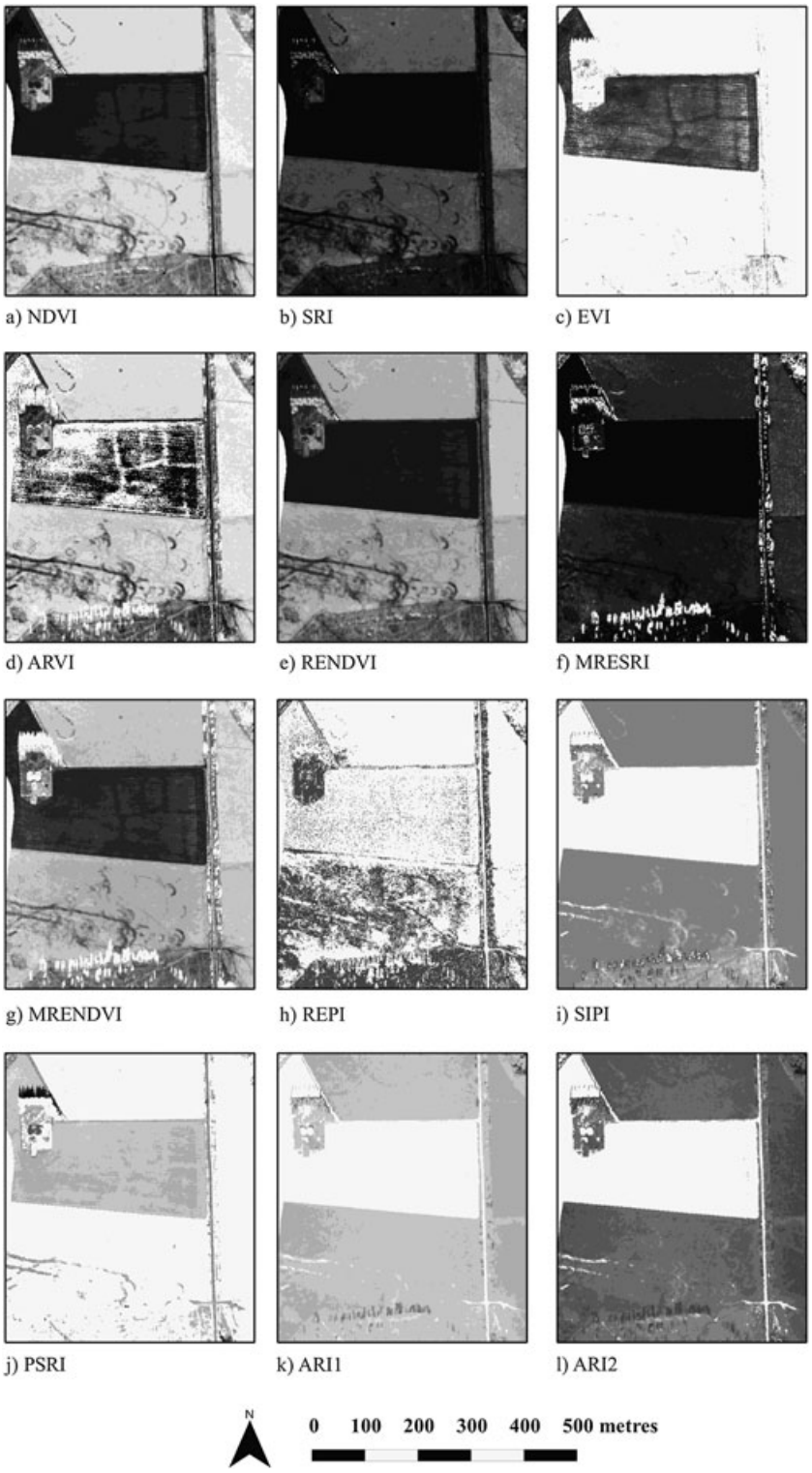

Figure 4. An extensive field system, running through three types of land use (from north to south: scheduled monument (grazed), heavily ploughed field, ungrazed grassland) as depicted in the vegetation indices.

DOI: 10.1002/arp

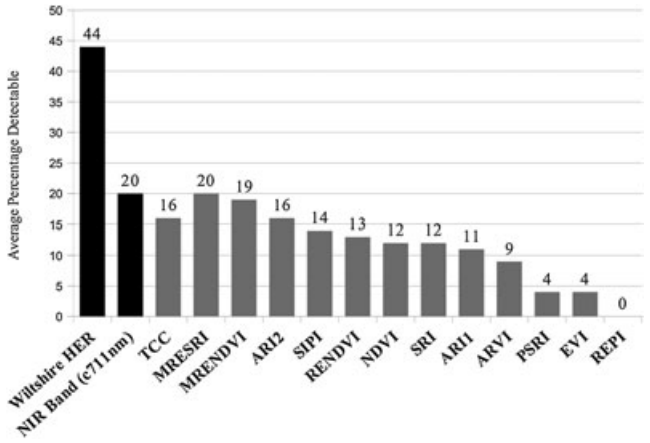

Figure 5. Average percentage feature length detection rates from the vegetation indices applied to the January spectral data.

seventh in January and ninth in May out of all the indices evaluated.

A comparison was made to see if the same features were being detected in the vegetation indices and the TCC (Table 3). This exercise demonstrated the complementarity of the different visualization techniques showing that the top performing vegetation indices recorded a significant number of extra features to the TCC of the same data. For example in the May data when the number of features recovered from the TCC, MRESRI and SRI was identical (40 features), the vegetation indices allowed the detection of at least 15 extra features that were not detectable in the TCC. The results from both the January and May data indicate that the use of the best performing vegetation index can lead to a 30–49% increase in feature detection over the TCC alone and a 24–30% increase over the best performing single band.

To summarize the usefulness of each of the indices more clearly with respect to the factors assessed, a ranked scoring system has been used to combine total number of features detected and level of complementarity to the TCC and best performing single band (Table 4).

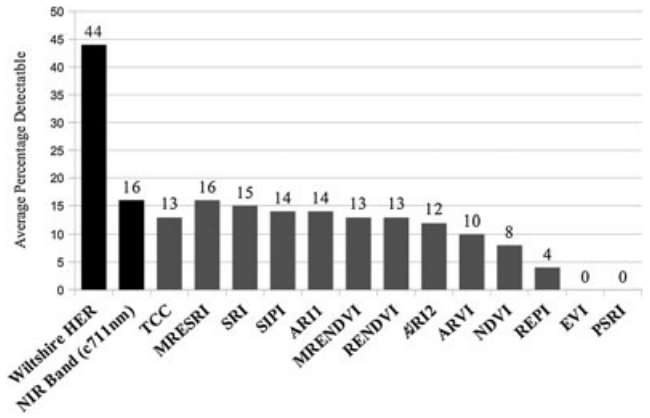

Figure 6. Average percentage feature length detection rates from the vegetation indices applied to the May spectral data.

Discussion

The results of a quantitative comparison of 12 indices selected for their empirical basis and applied to archive CASI spectral data showed that none of the indices gave detection rates comparable to those attained from transcription of the aerial photographic archive. Variation in feature detection rates relating to season was illustrated in this study, both in the TCC and vegetation indices, with more features being detectable in the January data than the May. Assessing the causes of this observed difference is complex due to the lack of contemporary ground observations, but it is suggested that the shallow root system of hardy vegetation such as grass is less likely to exhibit stress or variation associated with underlying archaeological features in its peak growing season (May) under non-drought conditions (such as were captured in the data used for this study).

The best performing indices varied across the spectral datasets of different dates, with only the MRESRI narrowband greenness index consistently performing well in this grassland environment. The study also illustrated that binary feature counts alone do not provide the best assessment of the usefulness of a particular index for archaeological prospection, as this measure does not quantify differences in the average percentage length of a feature that can be detected or the level of complementarity to the TCC in terms of additional features detected. An awareness of these factors, along with the quantitative comparison, will enable historic environment professionals to improve the application of vegetation indices. In summary, the best performing indices allowed the detection of a number of features that were not detectable in the TCC/best performing single band and therefore should be considered as complementary visualizations for archaeological feature detection.

Although it must be emphasized that the NDVI is a formula that can be applied to a number of band combinations in multispectral data and therefore there is no "standard" NDVI calculation, this study showed that the NDVI automatically calculated for these data by ENVI, was in fact one of the worst performing indices for archaeological feature detection. This is due to its use of a broad NIR band designed for satellite data when the spectral resolution of the airborne data lends

DOI: 10.1002/arp

Table 3. Comparison of complementarity or additional features detected by the vegetation indices over the TCC and best performing NIR band.

Vegetation index	Number of additional features when compared with				Increase in features detected when used as a secondary source to the TCC (%)		Increase in features detected when used as a secondary source to the NIR band (%)	
	January NIR band	January TCC	May NIR band	May TCC	January	May	January	May
MRESRI	14	22	11	15	49	38	25	24
MRENDVI	9	16	11	12	36	30	16	24
SIPI	7	15	14	15	33	38	13	31
ARI2	7	14	11	14	31	35	13	24
RENDVI	6	10	10	12	22	30	11	22
ARI1	6	10	10	11	22	28	11	22
SRI	6	9	13	16	20	40	11	29
ARVI	5	8	8	9	18	23	9	18
NDVI	5	8	9	9	18	23	9	20
EVI	1	2	0	0	4	0	2	0
PSRI	2	2	0	0	4	0	4	0
REPI	0	0	4	3	0	8	0	9

itself to more refined measures such as MRESRI and RENDVI. While it is clear that some indices can be used to detect archaeological features successfully, a lack of understanding of both spectral sensitivity and resolution often prevents the most appropriate indices from being applied.

Conclusions

This study provides the first quantitative analysis of vegetation indices derived from remotely sensed data in a grass-dominated environment. It was shown that a number of vegetation indices, particularly those in the narrow-band greenness category, are effective in detecting archaeological features. With hundreds of vegetation indices developed for environmental purposes, this study cannot be considered exhaustive, but it does indicate that appropriate selection of vegetation indices (based on spectral sensitivity of the target and resolution of the sensor) can enhance archaeological prospection from the use of the TCC composite or NIR band alone.

Acknowledgements

Archive CASI and ALS data were supplied by the Environment Agency. The authors would like to thank the Ministry of Defence and Defence Estates for facilitating access and especially Richard Osgood and Martin Brown, Senior Historic Environment Advisors. Access to the archaeological archive was facilitated by the staff of the Wiltshire HER and we are especially grateful for the expertise and encouragement of Roy Canham, former Wiltshire County Archaeologist. Gratitude is also expressed for the helpful comments of the two anonymous reviewers. The research is supported by a Bournemouth University Doctoral Research Bursary.

Table 4. Ranking of vegetation indices based on number of features and complementarity to other visualizations.

	January number of features	January TCC complementarity	January NIR complementarity	January final score	May number of features	May TCC complementarity	May NIR complementarity	May final score
MRESRI	12	12	12	36	11	10	9	30
MRENDVI	11	11	11	33	8	7	9	24
SIPI	9	10	9	28	10	10	12	32
ARI2	7	9	9	25	8	9	9	26
ARI1	9	7	7	23	6	6	6	18
RENDVI	7	7	7	21	8	7	6	21
SRI	5	6	7	18	11	12	11	34
NDVI	5	4	4	13	4	4	5	13
ARVI	4	4	4	12	5	4	4	13
PSRI	3	2	3	8	1	0	1	2
EVI	2	2	2	6	1	0	1	2
REPI	1	0	1	2	3	3	3	9

DOI: 10.1002/arp

References

Aqdus A, Hanson WS, Drummond J. 2012. The potential of hyperspectral and multi-spectral imagery to enhance archaeological cropmark detection: a comparative study. *Journal of Archaeological Science* **39**: 1915–1924.

Asner GP. 2008. *Vegetation Indices: ENVI Documentation*. ITT Visual Information Solutions.

Beck A, Philip G, Abdulkarim M, Donoghue D. 2007. Evaluation of Corona and Ikonos high resolution satellite imagery for archaeological prospection in western Syria. *Antiquity* **81**(311): 161–175.

Bennett RA. 2012. *Archaeological Remote Sensing: Visualisation and analysis of grass-dominated environments using airborne laser scanning and digital spectra data*. Unpublished PhD thesis, Bournemouth University.

Bennett R, Welham K, Hill RA, Ford A. 2011. Making the most of airborne remote sensing techniques for archaeological survey and interpretation. In *Remote Sensing for Archaeological Heritage Management*, Cowley DC (ed.). EAC Occasional Paper, Archaeolingua: Hungary; 99–107.

Brophy K, Cowley D (eds). 2005. *From the Air: Understanding Aerial Archaeology*. Tempus.

Challis K, Kincey M, Howard AJ. 2009. Airborne remote sensing of valley floor geoarchaeology using Daedalus ATM and CASI. *Archaeological Prospection* **16**(1): 17–33.

Curran PJ, Windham WR, Gholz HL. 1995. Exploring the relationship between reflectance red edge and chlorophyll concentration in slash pine leaves. *Tree Physiology* **15**: 203–206.

Datt B. 1999. A new reflectance index for remote sensing of chlorophyll content in higher plants: tests using *Eucalyptus* leaves. *Journal of Plant Physiology* **154**: 30–36.

Donoghue D, Shennan I. 1988. The application of remote sensing to environmental archaeology. *Geoarchaeology* **3**(4): 275–285.

English Heritage. 2006. *The National Mapping Programme Manual: A Methodology for the Use of Aerial Photographs for Archaeological Landscape Mapping and Analysis*. English Heritage: Swindon.

Gheyle W, Trommelmans R, Bourgeois J, *et al*. 2004. Evaluating CORONA: A case study in the Altai Republic (South Siberia). *Antiquity* **78**(300): 391–403.

Gitelson AA, Merzlyak MN. 1994. Spectral reflectance changes associated with autumn senescence of *Aesculus hippocastanum* L. and *Acer platanoides* L. Leaves. Spectral features and relation to chlorophyll estimation. *Journal of Plant Physiology* **143**: 286–92.

Gitelson AA, Merzlyak MN, Chivkunova OB. 2001. Optical properties and nondestructive estimation of anthocyanin content in plant leaves. *Photochemistry and Photobiology* **71**: 38–45.

Hejcman M, Ondracek J, Smrz Z. 2011. Ancient waste pits with wood ash irreversibly increase crop production in Central Europe. *Plant and Soil* **339**(1–2): 341–350.

Heute AR, Liu H, Batchily K, van Leeuwen W. 1997. A comparison of vegetation indices over a global set of TM images for EOS-MODIS. *Remote Sensing of Environment* **59**(3): 440–451.

Kaufman YJ, Tanre D. 1996. 'Strategy for direct and indirect methods for correcting the aerosol effect on remote sensing: from AVHRR to EOS-MODIS.' *Remote Sensing of Environment* **55**: 65–79.

Lasaponara R, Masini N. 2007. Detection of archaeological crop marks by using satellite QuickBird multispectral imagery. *Journal of Archaeological Science* **34**(2): 214–221.

Maxwell G (ed.). 1983. *The Impact of Aerial Reconnaissance on Archaeology*. Council for British Archaeology: London.

Merzlyak JR, Gitelson AA, Chivkunova OB, Rakitin VY. 1999. Non-destructive optical detection of pigment changes during leaf senescence and fruit ripening. *Physiologia Plantarum* **106**: 135–141.

Mumford G, Parcak S. 2002. Satellite image analysis and archaeological fieldwork in El-Markha Plain (South Sinai). *Antiquity* **76**(294): 953–954.

Pascucci S, Cavalli RM, Palombo A, Pignatti S. 2010. Suitability of CASI and ATM airborne remote sensing data for archaeological subsurface structure detection under different land cover: the Arpi case study (Italy). *Journal of Geophysics and Engineering* **7**(2): 183–189.

Penuelas J, Baret F, Filella I. 1995. Semi-empirical indices to assess carotenoids/chlorophyll-a ratio from leaf spectral reflectance. *Photosynthetica* **31**: 221–230.

Powlesland D, Lyall J, Hopkinson G, *et al*. 2006. Beneath the sand: remote sensing, archaeology, aggregates and sustainability: a case study from Heslerton, the Vale of Pickering, North Yorkshire, UK. *Archaeological Prospection* **13**(4): 291–299.

Ray TW. 1994. *A FAQ on Vegetation in Remote Sensing*. http://www.yale.edu/ceo/Documentation/rsvegfaq.html

Rouse JW, Haas RH, Schell JA, Deering DW. 1973. *Monitoring vegetation systems in the Great Plains with ERTS. Third ERTS Symposium*, NASA SP-351(I): 309–317.

Rowlands A, Sarris A. 2007. Detection of exposed and subsurface archaeological remains using multi-sensor remote sensing. *Journal of Archaeological Science* **34**(5): 795–803.

Sims DA, Gamon JA. 2002. Relationships Between Leaf Pigment Content and Spectral Reflectance Across a Wide Range of Species, Leaf Structures and Developmental Stages. *Remote Sensing of Environment* **81**: 337–354.

Traviglia A. 2005. *A semi-empirical index for estimating soil moisture from MIVIS data to identify sub-surface archaeological sites. 9a Conferenza Nazionale ASITA, Federazione delle Associazioni Scientifiche per le Informazioni Territoriali e Ambientali 15–18 novembre 2005, Centro Congressuale 'Le Ciminiere', Catania 2005 – Proceedings*.

Traviglia A. 2008. *The combinatorial explosion: defining procedures to reduce data redundancy and to validate the results of processed hyperspectral images*. In *Digital Discovery. Exploring New Frontiers in Human Heritage. CAA2006. Computer Applications and Quantitative Methods in Archaeology*, Rome.

Traviglia A, Cottica D. 2011. Remote sensing applications and archaeological research in the Northern Lagoon of Venice: the case of the lost settlement of Constanciacus. *Journal of Archaeological Science* **38**(9): 2040–2050.

DOI: 10.1002/arp

Tucker CJ. 1979. Red and photographic infrared linear combinations for monitoring vegetation. *Remote Sensing of Environment* **8**: 127–150.
Verhoeven G. 2012. Near-infrared aerial crop mark archaeology: from its historical use to current digital implementations. *Journal of Archaeological Method and Theory* **19**(1): 132–160.
Verhoeven G, Doneus M. 2011. Balancing on the borderline – a low-cost approach to visualise the red-edge shift for the benefit of aerial archaeology. *Archaeological Prospection* **18**(4): 267–278.
Verhoeven GJ, Smet PF, Poelman D, Vermeulen F. 2009. Spectral characterization of a digital still camera's NIR modification to enhance archaeological observation. *IEEE Transactions on Geoscience and Remote Sensing* **47**(10): 3456.
Wilkinson T. 1993. Linear hollows in the Jazira, Upper Mesopotamia. *Antiquity* **67**(256): 548–562.
Wilson DR (ed.). 1975. *Aerial reconnaissance for archaeology.* Council for British Archaeology: London.
Winterbottom SJ, Dawson T. 2005. Airborne multi-spectral prospection for buried archaeology in mobile sand dominated systems. *Archaeological Prospection* **12**(4): 205–219.

DOI: 10.1002/arp